Analysis of ordered arrays of adsorbed lysozyme by scanning tunneling microscopy

L. Haggerty and A. M. Lenhoff
Center for Molecular and Engineering Thermodynamics, Department of Chemical Engineering, University of Delaware, Newark, Delaware 19716 USA

ABSTRACT Scanning tunneling microscopy (STM) has been used to observe lysozyme at a graphite surface directly in order to gain mechanistic information about the molecular events involved in protein adsorption. The experiments were performed using an insulated tip in an aqueous protein solution, allowing the time course of the adsorption process to be followed, including the evolution of ordered arrays. Ordered arrays of protein molecules were observed, with lattice spacings that varied with bulk protein concentration and salt strength. Fourier analysis was used to determine the average cell dimensions of an array. From the observed lattice spacings, it was possible to estimate the surface coverage of the protein, and thus, by varying the conditions, adsorption isotherms could be obtained. These isotherms compare well with adsorption isotherms measured using total internal reflectance fluorescence (TIRF) spectroscopy on a hydrophobic surface. Since the protein is charged and the electrolyte has an effect on the isotherms, electrostatics are a likely controlling factor. Molecular electrostatics computations were thus used to investigate the possible origins of the lattice structure, and they suggest that favorable intermolecular interactions among adsorbed molecules are consistent with hydrophobically dominated protein-surface interactions.

INTRODUCTION

The extent of protein adsorption on surfaces can be measured in a number of different ways to generate adsorption isotherms. Generally, these techniques give a macroscopic view of adsorption; however, they do not provide much information on what is occurring at the molecular level. From bulk measurements, the average concentration of material on the surface can be measured, but how is this distributed? Are the molecules evenly spaced, or do they form aggregates and leave large bare patches? There are also many questions about the adsorption process that need to be answered, such as the time course of the process at the molecular level, and whether the molecules move once on the surface (there is evidence that surface diffusion occurs) (1, 2). More specific mechanistic questions involve the relative magnitudes of the protein-surface and protein-protein interactions that control the adsorption process. Answers to these questions cannot always be easily inferred from bulk measurements, and so a molecular approach is required. In this work, such insights are provided using scanning tunneling microscopy (STM).

Many biological species (DNA, membranes, proteins, etc.) have been observed by the STM with reasonably reproducible, consistent results, even though biological molecules are insulators (3). Using this technique, molecular resolution is possible both for dried protein films and for proteins adsorbed in liquid. We have previously observed that proteins in dried samples could readily be imaged with molecular resolution when there was high surface coverage, and that the molecules tend to form ordered arrays (4). A variety of other species, from proteins (4) and peptides (5) to inorganic polyanions (6) and "buckyballs" (7), form ordered arrays on surfaces as imaged by scanning probe microscopy. The formation of the two-dimensional arrays in dried films can be simply a result of the adsorption process; however, the drying process can have had some effect on the ordering. In order to investigate the phenomenon further and to gain more insight into the adsorption process, we undertook this work with the aim of observing the surface while the protein was still present in solution.

Qualitative information obtained from the images is very useful; however, if this is coupled with techniques such as computational image analysis, it is possible in addition to get quantitative information to characterize the images, such as the structure and lattice parameters of an array (8). Such data can, for example, be used to compare different images and to compare results from images to macroscopic data (e.g., surface coverages), in order to assess the consistency of the results. Quantitative information can also be used in conjunction with other techniques, both theoretical and experimental, to gain insight into the adsorption mechanism.

The image analysis tools needed in order to obtain quantitative information from the images are similar to those developed for the analysis of electron micrographs (9). Averaging techniques are especially effective for characterizing the data in an image of a two-dimensional crystal, e.g., providing unit cell information, since the molecules are ordered *a priori*. It can also be used to improve image resolution of low contrast micrographs.

The methods presented in this paper allow the STM to be used more effectively as an analytical tool, as we seek to show here for lysozyme. Lysozyme adsorption has been widely studied at both liquid-solid and liquid-air interfaces, as exemplified by several recent reports (10–13). While inferences have been drawn from these and other previous investigations regarding such issues as mo-

Address correspondence to A. M. Lenhoff.

0006-3495/93/03/886/10 $2.00

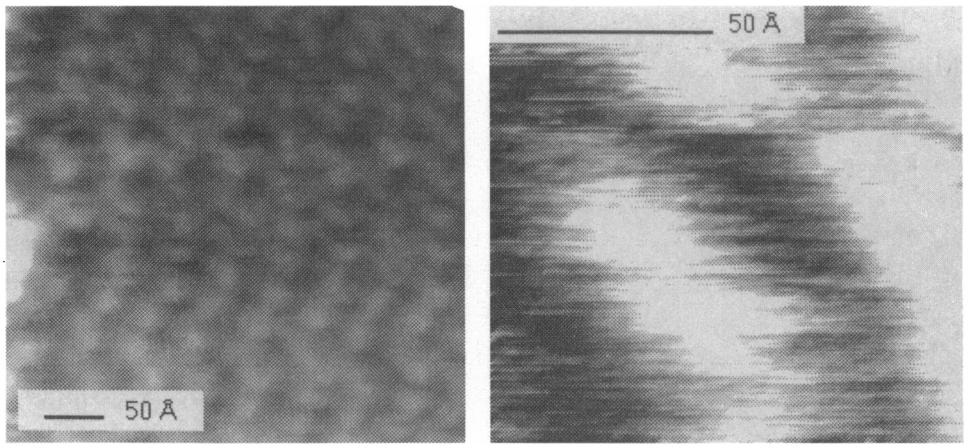

FIGURE 1 Images at different magnifications obtained after the initial adsorption period of lysozyme. Solution conditions: (*a*) (*left*) 8 mg/ml lysozyme, 0.1 M NaCl; (*b*) (*right*) 1 mg/ml lysozyme, no NaCl.

lecular packing and orientation at the interface, the results reported here show that STM studies can provide relevant molecular-level information directly, albeit not with sufficient resolution to address all outstanding questions.

MATERIALS AND METHODS

Aqueous solutions of hen egg-white lysozyme (L-6876; Sigma Chemical Co., St. Louis, MO) were used in the experiments. The crystal structure of lysozyme (molecular weight 13,930) indicates that the molecule has largest dimensions of $\sim 45 \times 30 \times 30$ Å and has a pronounced catalytic cleft (14). The solutions were buffered at pH 7 using a 0.01 M phosphate buffer solution and ranged in protein concentration from 0.1 to 10 mg/ml and in salt concentration from no salt to 1.0 M NaCl. A 200-μl cup that had a lower surface of highly ordered pyrolytic graphite (Union Carbide, Cleveland, OH) was used to hold the protein solution.

An LK Technologies (Bloomington, IN) STM 1000 was employed, using tips of Pt and Pt/Ir that were mechanically formed by cutting with sharp wire-cutters and then coated. The coating was applied by dipping the tip in nail polish (Revlon, Cover Girl) and then allowing it to dry in a vertical position, with the sharp end pointing upward in order to leave a small area at the very end of the tip uncoated to allow tunneling to take place (15). A few experiments were performed using electrochemically etched tips, and produced results that were consistent with those obtained using the mechanically cut tips. Scanning was performed in the constant-current mode, at a bias voltage of 50 mV and a current of 0.5–1 nA. Generally, the raw images were used for analysis; however, some post-image processing of the images, namely a low-pass filter to remove high frequency noise, was used for the images presented in the figures.

Fourier transforms of STM images were generated numerically in order to obtain power spectra showing the squared moduli of the Fourier coefficients. The FFTs were computed via the fast Hartley transform using *Image* 1.28b6, with extensions allowing frequency domain display and editing of gray scale images (image processing and analysis by Wayne Rasband, Research Services Branch, NIMH, National Institutes of Health; FFT code, 16).

Molecular electrostatics computations were performed in an effort to rationalize the structure of the adsorbed protein arrays, since electrostatics could be dominant and can be quite realistically modeled (17–20). The potential contours in and around the protein of interest, lyso-

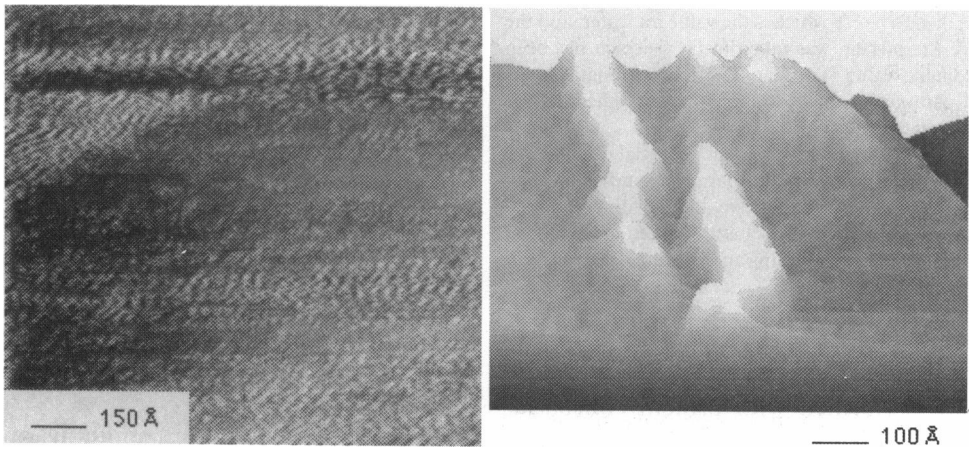

FIGURE 2 Images obtained during initial adsorption period. Solution conditions: (*a*) (*left*) 1 mg/ml lysozyme, no NaCl; (*b*) (*right*) 3 mg/ml lysozyme, 1 M NaCl.

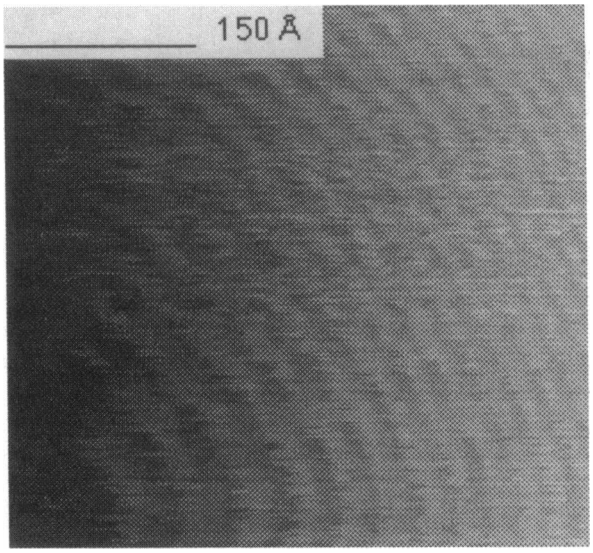

FIGURE 3 Example of the ring motif, which was observed at a wide range of protein and salt concentrations. Solution was 10 mg/ml lysozyme in 1 M NaCl.

zyme, in an electrolyte solution, were computed using the DelPhi program (21–23), a finite-difference procedure to find the electrostatic potential for an arbitrary three-dimensional geometry, with nonlinear effects due to the electrolyte included (24).

There were no adjustable parameters in the model used to calculate the potential contours. However, a number of system parameters were needed. The crystal structure of lysozyme was obtained from the Brookhaven Protein Data Bank (25). The charge distribution was set up using standard pK values (17) of the amino acid residues to determine if the residue would be charged at a given pH; the pK values for the amino and carboxy termini were also considered. The charge was placed on the nitrogen or oxygen atom that would be expected to be charged. If the charge was on a resonance structure, the charge was divided among multiple atoms, e.g., in glutamate and aspartate the charge was divided between the two oxygens. Since the likelihood of a charged atom falling exactly at a grid point is small, the DelPhi program assigns the charge to the eight surrounding grid points in proportion to their distance from the charge. The net charge of lysozyme calculated in this manner was consistent with measured values obtained from protein titration (26). The dielectric constant of the electrolyte solution was taken to be 80, which is the value for water, and the dielectric constant of the protein was taken to be 4, which has been shown to be a reasonable value (27, 23). The ionic strength enters directly as a system parameter, and is the key quantity affecting the thickness of the electrical double layer.

The calculations provide a three-dimensional potential distribution which accounts explicitly for protein molecular shape and charge distribution. Such a map shows areas of positive and negative potential that could interact in the formation of a closely packed array, and it thus provides a possible basis for quantifying and visualizing the electrostatic interactions.

RESULTS

Experiments were performed with protein concentrations that ranged from 0.1 to 10 mg/ml. Fig. 1 shows images obtained at different magnifications after the initial adsorption periods in the presence of solutions of lysozyme at 8 mg/ml with 0.1 M NaCl and 1 mg/ml with no NaCl. In both instances, roughly ellipsoidal molecules of ~40 Å in dimension are seen. Fig. 1 *a*, at lower magnification, shows the molecules to be packed in a structure that has considerable long-range order. However, no morphological details of the adsorbed protein molecules are readily discernible, even in Fig. 1 *b*, which is at a much higher magnification. The ordered structures are very similar to ones observed with dried samples of the same protein (4). In the dried samples it was not possible to tell if only a monolayer formed; however, for the samples in solution, the deposition process could be followed and only a monolayer was seen to form. This observation agrees with those using other techniques, such as total internal reflectance fluorescence (TIRF) spectroscopy, ellipsometry, and solution depletion, that show only monolayer coverage in most adsorption experiments at liquid-solid interfaces.

The arrays were produced without great difficulty or special provisions to ensure ordering, and their structural characteristics were reproducible. Artifacts are a problem in STM on graphite (28–30), so great care was taken to ensure reproducibility; thus micrographs for each set of conditions were recorded at different surface locations for a given experiment and for multiple experiments. Generally, comparable images for a specific set of conditions were recorded on a few different days, with fresh solutions, with new tips, and with freshly cleaved graphite. Clean graphite was imaged regularly to verify the scale of the pictures.

Some information on the formation of the adsorbed protein layer could be obtained from images gathered at short times after the solution was introduced (at most 20 min). Fig. 2 shows that images consistent with isolated molecules or incomplete arrays could sometimes be seen. It was relatively difficult to obtain good pictures at short times, probably because of the transient nature of the images and the possibility that the tip can mechanically move isolated molecules in the absence of other surface-bound molecules nearby to hinder such motion. Thus, the main emphasis in this work is on adsorption equilibrium.

A recurring theme in a number of the images was the presence of ring-like structures. Fig. 3 shows an example of this motif, which was observed at a wide range of protein and salt concentrations. The rings visible in the images were present in different orientations (i.e., the rings curved to the right, to the left and to the top and bottom), which suggests that this motif is not an artifact of the scanning mechanism. Although the rings are suggestive of growth of the adsorbate layer from a central nucleus, we have seen similar forms in scans of rod-like molecules, so the phenomenon requires further investigation.

The effect of solution conditions on micrographs of lysozyme is shown in Fig. 4, obtained using solutions at 1 and 5 mg/ml with no NaCl (Fig. 4, *a* and *b*) and at 5 mg/ml with 0.1 M NaCl (Fig. 4 *c*). Each image is at the

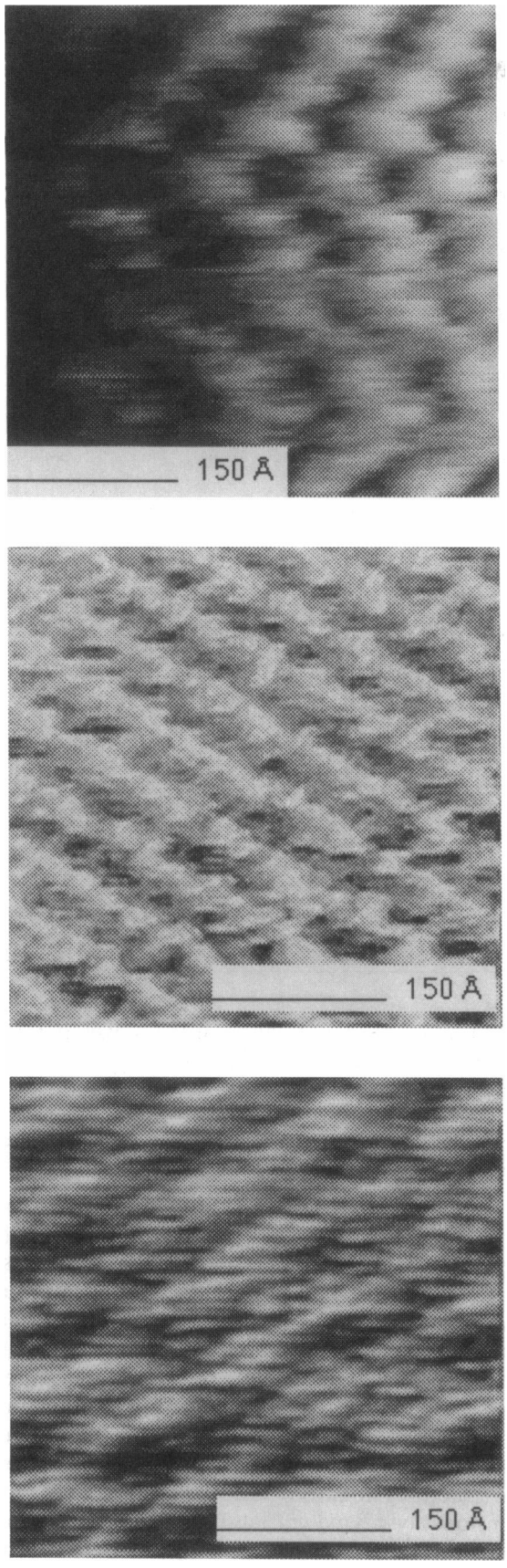

FIGURE 4 Effect of solution conditions on array structure of lysozyme. Solution conditions: (*a*) (*top*) 1 mg/ml lysozyme, no NaCl; (*b*) (*middle*) 5 mg/ml lysozyme, no NaCl; (*c*) (*bottom*) 5 mg/ml lysozyme, 0.1 M NaCl. All images are at the same magnification.

same magnification, thus allowing the lattice structures under the different conditions to be compared readily. Although the molecules seem to be of similar size, the lattice spacing of the array varies with both bulk protein concentration and salt concentration: the lattice spacing decreases as the bulk protein concentration is increased or the salt concentration decreased.

The Fourier transform of an image gives quantitative information about the dominant frequencies in the image, which can be used to construct an average unit cell for the array in the image. An example of a representative image and its Fourier transform, along with the reconstruction technique used, is shown in Fig. 5. This transform has four dominant peaks; four peaks are necessary to find the unit cell dimensions in real space. Sometimes the images had order in only one direction (i.e., only rows, and not individual molecules, were discernible), in which case there would be only two maxima, allowing the average row spacing to be determined. The Fourier transforms of the images usually had blurred maxima that were more elongated in the vertical direction than in the horizontal direction.

Fourier analysis of a number of images (Table 1) showed that the lattices were tetragonal with angles of ~60–80°. The average was 71.1° ± 5.9°. The lengths of the two sides varied with the solution characteristics, but their ratio remained between 1 and 1.6. The angle and the ratio of the sides did not seem to vary in any systematic way, but the lengths of the sides varied more systematically with bulk protein and salt concentration: the lengths of the sides decreased as bulk protein concentration increased or salt concentration decreased, by as much as a factor of 2.8 (see Table 1).

The lattice information obtained from the Fourier transforms can be used to find the area of the unit cell, which can then be used to calculate the local surface concentration; these results are also given in Table 1. Alternative local surface concentration estimates were made by measuring an average row spacing near the center of an STM micrograph. The local surface concentration was then obtained by assuming the molecules to be in a square array with the average lattice spacing given by the row spacing. These results are also given in Table 1 and are summarized in a plot of local surface concentration (Fig. 6 *a*). This plot shows that the surface concentration increases with bulk concentration until a plateau forms, with the level of the plateau decreasing as salt concentration increases; these trends are consistent with the images in Fig. 4. For example, with no added NaCl, the average row spacing decreased from 63.2 Å for a protein concentration of 0.1 mg/ml to 38.1 Å for 10 mg/ml. For a protein concentration of 5 mg/ml, the lattice spacing ranged from 38.8 Å for no added NaCl to 56.7 Å for 0.1 M NaCl to 65.4 Å for 1.0 M NaCl.

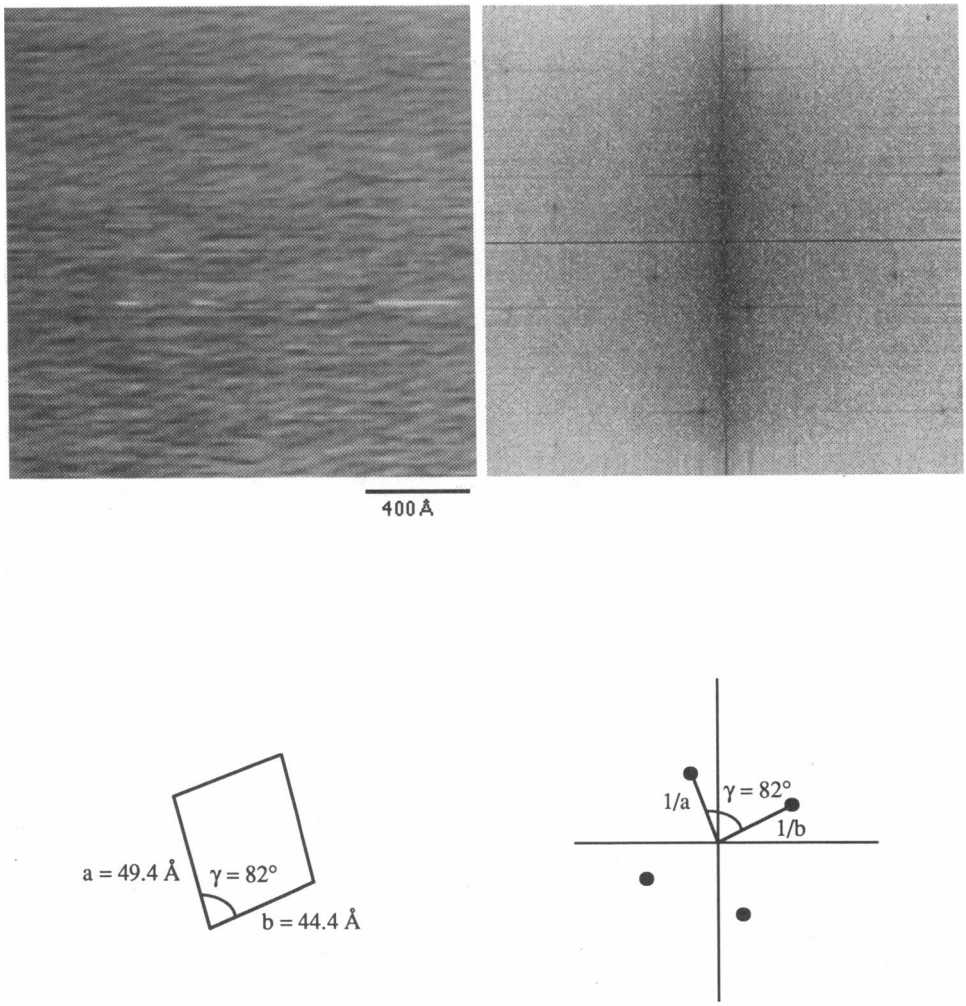

FIGURE 5 Representative image and its Fourier transform, along with reconstruction information. Solution was 5 mg/ml lysozyme in 0.1 M NaCl.

Higher-magnification images were more suited to direct measurement, while the lower-magnification images were more suited to the Fourier analysis since there were more repeat units in the field of view. If Fourier analysis was possible, then this method was used to obtain the average lattice dimensions of a micrograph since it should be more accurate; if the image was disordered and no sharp peaks were present in the Fourier space or if there were not enough unit cells in the image to distinguish the peaks from the average intensity of the image, which is present at the center of the transform, direct measurement was used. Generally, Fourier analysis was possible for only 1 or 2 images at a given set of conditions while many more images were amenable to row spacing measurement at each set of conditions (see Table 1). The results for both measurement techniques show good agreement in the trends they reflect. In addition, there is reasonable quantitative agreement in the absolute values of the surface coverage, with the largest relative discrepancies at low surface coverages, where absolute errors are quite small and where image acquisition was more difficult (see below). The square-lattice assumption made in calculating surface coverage based on the row spacing obviously also contributes to the discrepancies.

DISCUSSION

The images of the proteins in liquid are not as well resolved as the images of dried protein films reported previously (4). However, molecular resolution that is adequate for analysis was still obtained. Since the wet and dry images show similar structures, it is possible that the same mechanism is driving the formation of the structures, with self-assembly into ordered arrays occurring as a natural part of the adsorption process. Incomplete arrays such as those shown in Fig. 2 suggest that self-assembly proceeds by nucleation and growth, with island-like structures similar to those seen in growth of three-dimensional lysozyme crystals (31). Aggregation in solution may play a role, especially at higher lysozyme concentrations, where especially dimers are known to form (32). These observations suggest a role for favorable protein-protein interactions, an aspect to which we

TABLE 1 **Characteristics of ordered arrays of lysozyme on graphite**

Protein concentration	Salt concentration	*a*	*b*	*a/b*	Angle	Surface concentration		Difference
							$\mu g/cm^2$	
[*mg/ml*]	[*M NaCl*]	[*Å*]	[*Å*]		[°]	*FFT data*	*Average row spacing**	[%]
0.1	0	62.5	48.6	1.29	68	0.082	0.058 ± 0.016 (15)	41.4
1	0	67.4	48.6	1.39	70	0.075	0.089 ± 0.015 (5)	15.7
3	0	60.0	48.6	1.23	67	0.086	0.109 ± 0.028 (7)	21.1
5	0	48.0	34.0	1.41	66	0.155	0.154 ± 0.027 (9)	0.6
8	0	41.8	36.4	1.15	63	0.171	0.147 ± 0.042 (4)	16.3
10	0	43.8	36.5	1.20	61	0.165	0.159 ± 0.033 (28)	3.8
0.1	0.1	134.8	125.1	1.08	72	0.014	0.026 ± 0.007 (8)	46.2
1	0.1	67.4	62.6	1.08	74	0.057	0.076 ± 0.010 (8)	25.0
3	0.1	64.9	51.1	1.27	83	0.070	0.072 ± 0.003 (4)	2.8
5	0.1	49.4	44.4	1.11	82	0.107	0.077 ± 0.018 (6)	39.0
8	0.1	51.2	41.2	1.24	76	0.113	0.102 ± 0.037 (8)	10.8
10	0.1	58.4	40.0	1.46	67	0.108	0.109 ± 0.024 (15)	0.9
0.1	1	159.3	146.0	1.09	68	0.011	0.021 ± 0.004 (5)	47.6
1	1	73.0	62.5	1.17	72	0.053	0.036 ± 0.005 (8)	47.2
3	1	81.6	51.4	1.59	69	0.059	0.059 ± 0.013 (4)	0
5	1	93.2	58.3	1.60	77	0.044	0.054 ± 0.013 (9)	18.5
8	1	55.5	46.2	1.20	75	0.093	0.087 ± 0.039 (8)	6.9
10	1	73.0	48.7	1.50	69	0.070	0.068 ± 0.008 (12)	2.9

* Figure in parentheses denotes number of images used in calculating the surface concentration.

return later. It is, however, possible that incomplete arrays are more likely to be seen than isolated molecules simply because the latter are more difficult to image, as discussed in the following paragraphs.

While the equilibrium images of full arrays were fairly easily obtained, images at low surface coverages, which occur at high salt concentrations and low bulk protein concentrations or at short times, were more troublesome, presumably due to mobility of the protein molecules. It appears that the protein-protein interactions that result when the proteins are packed reasonably closely in arrays are important for obtaining a stable image. Movement of the molecules by only a few Ångströms would cause disturbances in the image and would seriously hinder resolution. A corollary to this observation is that the resolution under water would not be as good as resolution of dried films because of the additional mobility that is possible in solution.

In view of these sources of uncertainty in the images, it is important to note that the results obtained were consistent. The molecules were generally globular and of similar size, and their dimensions were consistent with crystal structure data for lysozyme. The long-range order that is observed in the micrographs indicates that, at least in this system, proteins can adsorb by forming a two-dimensional array. Since no atomic detail or even morphological detail (e.g., the cleft in lysozyme) could be conclusively observed, it is impossible to say whether these arrays are in fact crystalline. However, the lattice spacings of the arrays were all replicated and were consistent. Moiré patterns are a known artifact of STM on graphite (29); however, the spacing of the Moiré pattern would not fortuitously coincide with the size of the protein molecule in scores of experiments, both dried and in liquid. In addition, when the experiments began, there was no adsorption and the underlying graphite was imaged. Thus, the ordered structures were clearly associated with the protein adsorbate. Although the lattice dimensions obtained were consistent with molecular dimensions, the resolution was not sufficient to allow definitive determination of adsorption orientation.

Although the Fourier transform of the image gives much more detailed information about the lattice, not all of the images are suitable for Fourier analysis. First, a large number of repeat units is needed. Large repeat distances (relative to the size of the image) result in peaks that are very close to the origin in frequency space, and it is very difficult to resolve these peaks, mainly since the average intensity of the image is at the origin and this large peak and its intensity can overwhelm peaks that are very close to it. In addition, the peak intensity will be low since there are not enough objects to average. Second, the molecules must be ordered: the power spectra will show merely noise even for very well resolved molecules if they are in a totally random arrangement. All of the images in this study showed a degree of disorder, which led to some noise in frequency space; however, peaks corresponding to the lattice spacing were usually perceptible.

In most of the images obtained here, the lateral resolution was better than the vertical resolution, due to the scanning mechanism; therefore oblique or vertical rows of molecules are the dominant feature. That the row orientation varied among the images seen is evidence that ordering was not a result of the scanning process. These rows lead to two dominant peaks in the frequency do-

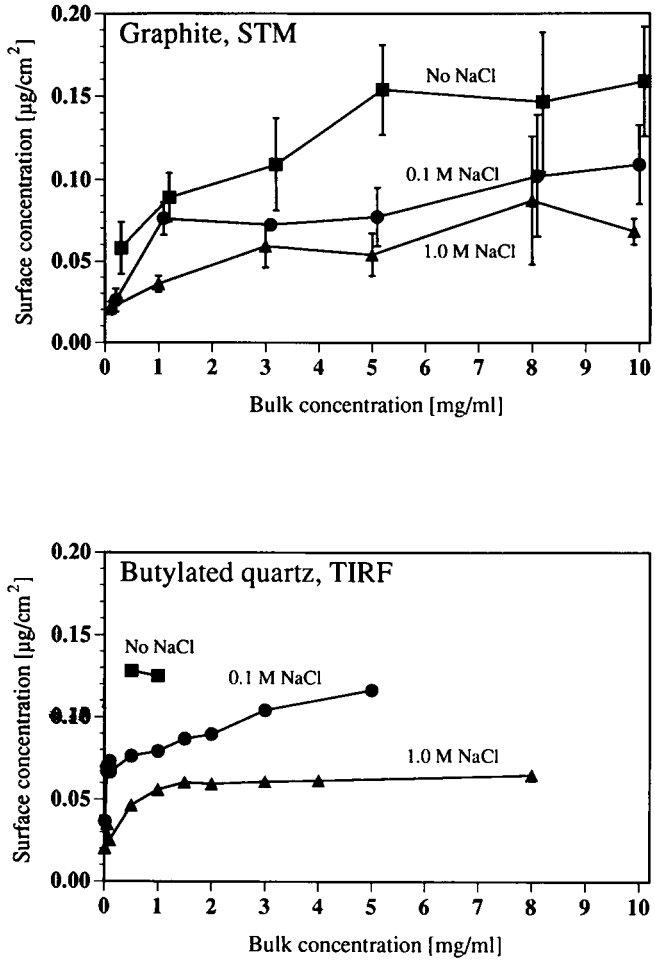

FIGURE 6 Adsorption isotherms showing salt effects on surface coverage of lysozyme. Results obtained by: (*a*) (*top*) STM on highly oriented pyrolytic graphite; (*b*) (*bottom*) TIRF spectroscopy on butylated quartz (Shibata and Lenhoff, 1992).

main. The disorder in the vertical direction caused the maxima in frequency space to appear as vertically smeared spots that sometimes cover the entire vertical frequency range. However, for the best images (where vertical resolution is comparable to lateral resolution and where the globular shape of the molecules is more readily discernible), other peaks appear in the frequency domain. The locations of these peaks were used to obtain the dimensions of the unit cell.

In the adsorption isotherms obtained from the row spacing in the STM images (Fig. 6), the error bars on the points are somewhat large; however, this is to be expected from a local measurement, especially when counting molecules from a few micrographs. The square-lattice assumption is also a contributing factor. It is nevertheless notable that the results compare well with adsorption isotherms measured using other techniques. Fig. 6 compares the results from the STM (Fig. 6 *a*) with results using TIRF spectroscopy (13) (Fig. 6 *b*). The TIRF results were also obtained on a hydrophobic surface (butylated quartz) and used the same protein (lysozyme), salt (NaCl), and buffer (pH 7). The isotherms exhibit the same trends and the absolute surface concentrations are in fairly good agreement, reaching plateaus that approach a level of monolayer coverage. Monolayer coverage of lysozyme molecules can be estimated from the dimensions of the molecule to be between 0.16 and 0.27 $\mu g/cm^2$, depending on the adsorption orientation (12).

The effect of protein concentration in the isotherms is simply a mass action one, while electrostatic interactions are the likely factor governing the trend with salt. Since the graphite surface is uncharged, a colloid science approach to understanding the salt effect implicates mainly protein-protein interactions in solution and on the surface. The mechanistic basis can be sought from either of two points of view. The simpler considers just the net charge on the protein, which for lysozyme is about +8 at pH 7 (26). At first sight it may seem that intermolecular repulsion may assist in array formation, as it does in leading to ordered three-dimensional structures of charged or uncharged colloidal particles (33). However, the situation is more complex here. Protein-protein repulsion must be overcome in order for adsorption to occur, especially at low ionic strengths, where the molecules are most closely packed on the surface despite the fact that the double layers around the molecules are relatively thick. At higher ionic strengths, the repulsion between protein molecules should be weaker due to the screening from the condensed double layer, and it would be expected that this reduction in the electrostatic interactions would result in closer packing of the molecules on the surface. That this is not observed suggests that protein-protein and protein-salt interactions in solution, which control the protein chemical potential and solubility, are more important. This role of salting-in has previously been used to explain salt effects on protein adsorption trends (34, 13).

The alternative view of the electrostatic effects goes beyond simply the net charge, and takes into account the anisotropy of the charge distribution on the protein, coupled with the ordered structure of the arrays. These considerations suggest the possibility of favorable protein-protein interactions on the surface if the molecules are packed in an appropriate orientation. In order to assess this issue in the light of the lattice structures observed, the electrostatic potential distributions in and around a single lysozyme molecule in electrolyte solutions with the same ionic strength as those used in the experiments were generated using DelPhi, as described earlier. Two-dimensional cross-sectional contour maps were generated for planes through the molecule in a spectrum of orientations and a range of ionic strengths.

Two extreme results at 0.01 M ionic strength are shown; results at higher ionic strengths are similar, apart from their thinner double layers. Fig. 7 *a* shows an orientation in which a fairly constant positive potential

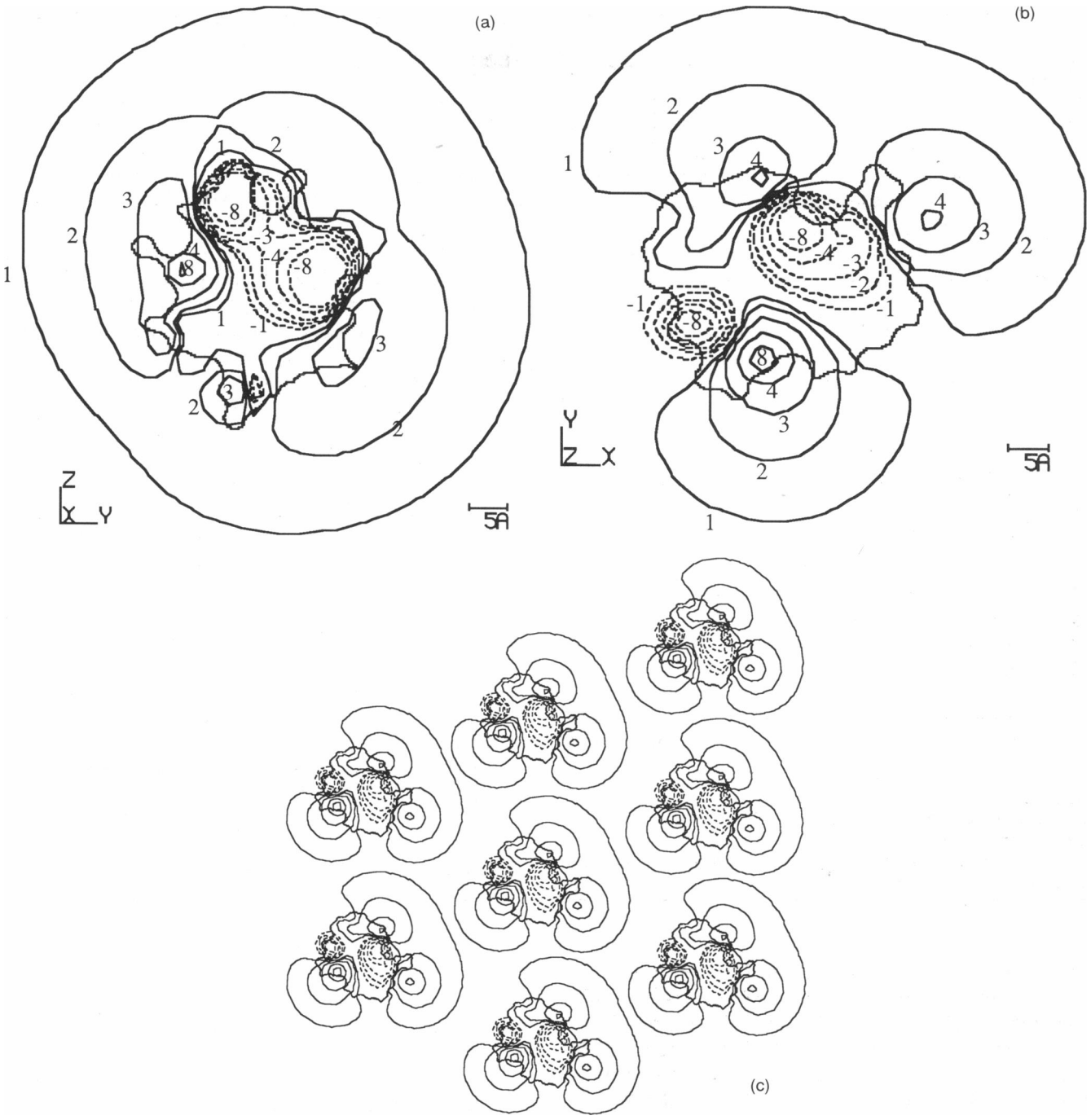

FIGURE 7 Electrostatic potential contours (units of kT/e; 1 kT/e = 25.7 mV) through the center of a lysozyme molecule at pH 7 and 0.01 M ionic strength. Molecule oriented with the face containing the active site (*a*) perpendicular to the page, (*b*) parallel to the page. (*c*) Multiple molecules oriented as in b configured into a tetragonal packing with angle suggested by the frequency space data shown in Table 1.

surrounds the protein molecule; electrostatic interactions between multiple molecules in this configuration would generally result in repulsion. However, Fig. 7 *b* shows another configuration, in which positive and negative potentials each exist at different locations in the solution around the molecule. It is possible that, in this configuration, multiple molecules could interact favorably with each other. In fact, it is feasible to fit these contours into a tetragonal packing with an angle suggested by the frequency space data (Fig. 7 *c*), in which the protein-protein interactions along one axis are clearly favorable. It is interesting to note that in this orientation the face of the molecule in which the active site appears is parallel to the plane of the page; thus adsorption in this orientation would require this face or the one opposite it to be in contact with the surface. This is con-

sistent with the arguments of Horsley et al. (10), whose molecular graphics analysis of the surface residues of lysozyme suggests that lysozyme adsorption on hydrophobic surfaces may well occur via a hydrophobic patch present on the face opposite the active site. Another consequence of a favorable contribution to protein-protein interactions is that this would provide a driving force for array formation by nucleation and growth, as discussed earlier in the context of Fig. 2.

Use of potentials around a single, isolated molecule to analyze array structure is simplistic in view of the double-layer overlap that would occur in an actual array. In addition, we have no evidence at present of orientational order in the arrays such as is shown in Fig. 7 *c*, although one could, of course, exploit more degrees of freedom in seeking favorable interactions by allowing different molecules to have different orientations, even in an ordered array (i.e., by having more than one molecule per unit cell, as in a three-dimensional lysozyme crystal). Nonetheless, Fig. 7 *c* suggests that the nonuniform charge distribution within the molecule allows unfavorable interactions on the surface to be reduced. It is possible that the interactions indeed become favorable, but determining whether this is the case requires more detailed computations, including consideration of other effects such as van der Waals and hydration interactions, on which the influence of ionic strength is poorly understood. These matters, and assessment of the contribution of protein-surface interactions, are beyond the scope of this paper.

SUMMARY

STM has been used to show that lysozyme adsorbed on graphite self-assembles into two-dimensional arrays with considerable long-range order. The surface coverages obtained as a function of protein and salt concentrations agree well with results obtained by TIRF on a different hydrophobic surface, suggesting that such two-dimensional ordering is a more general phenomenon in the adsorption process. The mechanisms driving self-assembly and lattice structure, especially spacing dimensions, remain to be established, but the salt effects observed indicate that electrostatics are implicated. That surface coverage decreases with increasing salt concentration can be explained either by the lower protein activity coefficient with increasing ionic strength (salting-in), or by the contribution of favorable electrostatic interactions due to the anisotropic charge distribution on the protein. The molecular-level information accessible both experimentally, by STM, and theoretically, such as by molecular electrostatics computations, can be crucial in resolving issues such as these, and in elucidating protein adsorption mechanisms in general.

We thank J. M. Schultz for useful discussions, and the National Science Foundation (CBT-8657185) and the National Aeronautics and Space Administration (NAGW-2798) for financial support.

Received for publication 11 August and in final form 1 November 1992.

REFERENCES

1. Tilton, R. D., A. P. Gast, and C. R. Robertson. 1990. Surface diffusion of interacting proteins. Effect of concentration on the lateral mobility of adsorbed bovine serum albumin. *Biophys. J.* 58:1321–1326.
2. Tilton, R. D., C. R. Robertson, and A. P. Gast. 1990. Lateral diffusion of bovine serum albumin adsorbed at the solid-liquid interface. *J. Coll. Interf. Sci.* 137:192–203.
3. Engel, A. 1991. Biological applications of scanning probe microscopes. *Annu. Rev. Biophys. Biophys. Chem.* 20:79–108.
4. Haggerty, L., B. A. Watson, M. A. Barteau, and A. M. Lenhoff. 1991. Ordered arrays of proteins on graphite observed by scanning tunneling microscopy. *J. Vac. Sci. Technol.* B9:1219–1222.
5. Miles, M. J., T. McMaster, H. J. Carr, A. S. Tatham, P. R. Shewry, J. M. Field, P. S. Belton, D. Jeenes, B. Hanley, M. Whittam, P. Cairns, V. J. Morris, and N. Lambert. 1990. Scanning tunneling microscopy of biomolecules. *J. Vac. Sci. Technol.* A8:698–702.
6. Watson, B. A., M. A. Barteau, L. Haggerty, A. M. Lenhoff, and R. S. Weber. 1992. Scanning tunneling microscopy and tunneling spectroscopy of ordered hetero- and iso-polyacid arrays on graphite. *Langmuir.* 8:1145–1148.
7. Li, Y. Z., J. C. Patrin, M. Chander, J. H. Weaver, L. P. F. Chibante, and R. E. Smalley. 1991. Ordered overlayers of C_{60} on GaAs(110) studied with scanning tunneling microscopy. *Science (Wash. DC).* 252:547–548.
8. Garnaes, J., D. K. Schwartz, R. Viswanathan, and J. A. N. Zasadzinski. 1992. Domain boundaries and buckling superstructures in Langmuir-Blodgett films. *Nature (Lond.).* 357:54–57.
9. Misell, D. L. 1978. Image Analysis, Enhancement and Interpretation. North-Holland, Amsterdam.
10. Horsley, D., J. Herron, V. Hlady, and J. D. Andrade. 1987. Human and hen lysozyme adsorption: a comparative study using total internal reflection fluorescence spectroscopy and molecular graphics. *In* Proteins at Interfaces: Physical and Biochemical Studies. J. L. Brash and T. A. Horbett, editors. ACS Symposium Series, Vol. 343. American Chemical Society, Washington, DC. 290–305.
11. Arai, T., and W. Norde. 1990. The behavior of some model proteins at solid-liquid interfaces. 1. Adsorption from single protein solutions. *Coll. Surf.* 51:1–15.
12. Hunter, J. R., P. K. Kilpatrick, and R. G. Carbonell. 1990. Lysozyme adsorption at the air/water interface. *J. Coll. Interf. Sci.* 137:462–482.
13. Shibata, C. T., and A. M. Lenhoff. 1992. TIRF of salt and surface effects on protein adsorption. I. Equilibrium. *J. Coll. Interf. Sci.* 148:469–484.
14. Blake, C. C. F., G. A. Mair, A. C. T. North, D. C. Phillips, and V. R. Sarma. 1967. On the conformation of the hen egg-white lysozyme molecule. *Proc. Roy. Soc.* B167:365–377.
15. Gewirth, A. A., D. H. Craston, and A. J. Bard. 1989. Fabrication and characterization of microtips for in situ scanning tunneling microscopy. *J. Electroanal. Chem.* 261:477–482.
16. Reeves, A. A. 1990. Optimized fast Hartley transform for the MC68000 with applications in image processing. Master of Science Thesis, Thayer School of Engineering, Dartmouth College, NH.
17. Matthew, J. B. 1985. Electrostatic effects in proteins. *Annu. Rev. Biophys. Biophys. Chem.* 14:387–417.

18. Rogers, N. K. 1986. The modelling of electrostatic interactions in the function of globular proteins. *Prog. Biophys. Mol. Biol.* 48:37–66.
19. Harvey, S. 1989. Treatment of electrostatic effects in macromolecular modeling. *Proteins.* 5:78–92.
20. Sharp, K., and B. Honig. 1990. Electrostatic interactions in macromolecules: Theory and applications. *Annu. Rev. Biophys. Biophys. Chem.* 19:301–332.
21. Klapper, I., R. Hagstrom, R. Fine, K. Sharp, and B. H. Honig. 1986. Focusing of electric fields in the active site of Cu-Zn superoxide dismutase: effects of ionic strength and amino-acid modification. *Proteins.* 1:47–59.
22. Gilson, M. K., K. A. Sharp, and B. H. Honig. 1987. Calculating the electrostatic potential of molecules in solution: Method and error assessment. *J. Comput. Chem.* 9:327–335.
23. Gilson, M. K., and B. H. Honig. 1988. Calculation of the total electrostatic energy of a macromolecular system: solvation energies, binding energies, and conformational analysis. *Proteins.* 4:7–18.
24. Jayaram, B., K. Sharp, and B. H. Honig. 1989. The electrostatic potential of B-DNA. *Biopolymers.* 28:975–993.
25. Bernstein, F. C., T. F. Koetzle, G. J. B. Williams, E. F. Meyer, M. D. Brice, J. R. Rodgers, O. Kennard, T. Shimanouchi, and M. J. Tasumi. 1977. The Protein Data Bank: a computer-based archival file for macromolecular structures. *J. Mol. Biol.* 112:535–542.
26. Tanford, C., and R. Roxby. 1972. Interpretation of protein titration curves. Application to lysozyme. *Biochemistry.* 11:2192–2198.
27. Harvey, S. C., and P. Hoekstra. 1972. Dielectric relaxation spectra of water adsorbed on lysozyme. *J. Phys. Chem.* 76:2987–2994.
28. Clemmer, C. R., and T. P. Beebe. Graphite: A mimic for DNA and other biomolecules in scanning tunneling microscope studies. 1991. *Science (Wash. DC.).* 251:640–642.
29. Liu, C. Y., H. Chang, and A. J. Bard. 1991. Large scale hexagonal domainlike structures superimposed on the atomic corrugation of a graphite surface observed by scanning tunneling microscopy. *Langmuir.* 7:1138–1142.
30. Chang, H., and A. J. Bard. 1991. Observation and characterization by scanning tunneling microscopy of structures generated by cleaving highly oriented pyrolytic graphite. *Langmuir.* 7:1143–1153.
31. Durbin, S. D., and G. Feher. 1990. Studies of crystal growth mechanisms of proteins by electron microscopy. *J. Mol. Biol.* 212:763–774.
32. Sophianopoulos, A. J., and K. E. Van Holde. 1964. Physical studies of muramidase (lysozyme). II. pH-dependent dimerization. *J. Biol. Chem.* 239:2516–2524.
33. Russel, W. B., D. A. Saville, and W. R. Schowalter. 1989. Colloidal Dispersions. Cambridge University Press, Cambridge. 338–348.
34. Melander, W., and C. Horváth. 1977. Salt effects on hydrophobic interactions in precipitation and chromatography of proteins: an interpretation of the lyotropic series. *Arch. Biochem. Biophys.* 183:200–215.